J|A|C|S ARTICLES

Published on Web 07/07/2010

Controlled Incorporation of Particles into the Central Portion of Vesicle Walls

Yiyong Mai and Adi Eisenberg*

Department of Chemistry, McGill University, 801 Sherbrooke Street West, Montreal, Quebec, H3A 2K6, Canada

Received March 22, 2010; E-mail: adi.eisenberg@mcgill.ca

Abstract: Vesicles have attracted considerable attention recently because of many potential applications as well as intrinsic interest in the structures. The incorporation of various particles into vesicle walls has also received attention. One of the unsolved problems, in this context, is the controlled incorporation of particles into only the central portion of the vesicle walls, i.e. approximately halfway between the external and internal interfaces. In this paper, we describe a general method for the incorporation of particles into only the central portion, i.e. central 10−20%, of the vesicle walls. The strategy involves the use, as coatings on the particles, of diblock copolymers of a structure similar to that of the vesicle formers, which allows the particles to be preferentially localized in the central portion of the walls.

1. Introduction

Block copolymer vesicles, prepared by supermolecular self-assembly of amphiphilic block copolymers in selective solvents, have attracted considerable attention due to the number of potential applications in the pharmaceutical, medical, and catalysis fields, as well as the academic interest in such structures,[1−24] which are frequently referred to as polymersomes.[4] Some of the applications are related to the increased thickness, rigidity, and stability of the vesicle membranes compared to those of classical liposomes.[4,5] The potential applications of vesicles mostly rely on the presence of hydrophilic cavities, which offer a possibility for the encapsulation of various hydrophilic substances.[25−35] Vesicle wall incorporation is another important issue, because it may open up additional potential applications for vesicles by permitting the simultaneous incorporation of particles into vesicle walls, e.g. hydrophobic, labeled, or catalytic species, such as quantum dots (QDs), along with the hydrophilic species in the cavities.

For the reasons mentioned above, the incorporation of particles into vesicle walls has attracted considerable interest, and a number of attempts have been made to achieve it in spite

(1) van Hest, J. C. M.; Delnoye, D. A. P.; Baars, M. W. P. L.; van Genderen, M. H. P.; Meijer, E. W. *Science* **1995**, *268*, 1592–1595.
(2) Zhang, L. F.; Eisenberg, A. *Science* **1995**, *268*, 1728–1731.
(3) Zhang, L. F.; Yu, K.; Eisenberg, A. *Science* **1996**, *272*, 1777–1779.
(4) Discher, B. M.; Won, Y. Y.; Ege, D. S.; Lee, J. C. M.; Bates, F. S.; Discher, D. E.; Hammer, D. A. *Science* **1999**, *284*, 1143–1146.
(5) Discher, D. E.; Eisenberg, A. *Science* **2002**, *297*, 967–973.
(6) Chécot, F.; Lecommandoux, S.; Gnanou, Y.; Klok, H. *Angew. Chem., Int. Ed.* **2002**, *41*, 1339–1343.
(7) Jain, S.; Bates, F. S. *Science* **2003**, *300*, 460–464.
(8) Du, J. Z.; Chen, Y. M.; Zhang, Y. H.; Han, C. C.; Fischer, K.; Schmidt, M. *J. Am. Chem. Soc.* **2003**, *125*, 14710–14711.
(9) Antonietti, M.; Förster, S. *Adv. Mater.* **2003**, *15*, 1323–1333.
(10) Binder, W. H.; Barragan, V.; Menger, F. M. *Angew. Chem., Int. Ed.* **2003**, *42*, 5802–5827.
(11) Zhou, Y. F.; Yan, D. Y. *Angew. Chem., Int. Ed.* **2004**, *43*, 4896–4899.
(12) Uzun, O.; Sanyal, A.; Nakade, H.; Thibault, R. J.; Rotello, V. M. *J. Am. Chem. Soc.* **2004**, *126*, 14773–14777.
(13) Ghoroghchian, P. P.; Frail, P. R.; Susumu, K.; Blessington, D.; Brannan, A. K.; Bates, F. S.; Chance, B.; Hammer, D. A.; Therien, M. J. *Proc. Natl. Acad. Sci. U.S.A.* **2005**, *102*, 2922–2927.
(14) Chen, D. Y.; Jiang, M. *Acc. Chem. Res.* **2005**, *38*, 494–502.
(15) Vriezema, D. M.; Aragones, M. C.; Elemans, J.; Cornelissen, J.; Rowan, A. E.; Nolte, R. J. M. *Chem. Rev.* **2005**, *105*, 1445–1489.
(16) Li, Y. T.; Lokitz, B. S.; McCormick, C. L. *Angew. Chem., Int. Ed.* **2006**, *45*, 5792–5795.
(17) Li, Z. B.; Hillmyer, M. A.; Lodge, T. P. *Nano Lett.* **2006**, *6*, 1245–1249.
(18) Mai, Y. Y.; Zhou, Y. F.; Yan, D. Y. *Small* **2007**, *3*, 1170–1173.
(19) Kumar, M.; Grzelakowski, M.; Zilles, J.; Clark, M.; Meier, W. *Proc. Natl. Acad. Sci. U.S.A.* **2007**, *104*, 20719–20724.
(20) Sundararaman, A.; Stephan, T.; Grubbs, R. B. *J. Am. Chem. Soc.* **2008**, *130*, 12264–12265.
(21) Blanazs, A.; Armes, S. P.; Ryan, A. J. *Macromol. Rapid Commun.* **2009**, *30*, 267–277.
(22) Howse, J. R; Jones, R. A. L.; Battaglia, G.; Ducker, R. E.; Leggett, G. J.; Ryan, A. J. *Nat. Mater.* **2009**, *8*, 507–511.
(23) Kim, A. J.; Kaucher, M. S.; Davis, K. P.; Peterca, M.; Imam, M. R.; Christian, N. A.; Levine, D. H.; Bates, F. S.; Percec, V.; Hammer, D. A. *Adv. Funct. Mater.* **2009**, *19*, 2930–2936.
(24) Sun, G. R.; Fang, H. F.; Cheng, C.; Lu, P.; Zhang, K.; Walker, A. V.; Taylor, J. A.; Wooley, K. L. *ACS Nano* **2009**, *3*, 673–681.
(25) Ding, J. F.; Liu, G. J. *J. Phys. Chem. B* **1998**, *102*, 6107–6113.
(26) Discher, B. M.; Hammer, D. A.; Bates, F. S.; Discher, D. E. *Curr. Opin. Colloid Interface Sci.* **2000**, *5*, 125–131.
(27) Rosler, A.; Vandermeulen, G. W. M.; Klok, H. *Adv. Drug Delivery Rev.* **2001**, *53*, 95–108.
(28) Vriezema, D. M.; Hoogboom, J.; Velonia, K.; Takazawa, K.; Christianen, P. C. M.; Maan, J. C.; Rowan, A. E.; Nolte, R. J. M. *Angew. Chem., Int. Ed.* **2003**, *42*, 772–776.
(29) Bellomo, E. G.; Wyrsta, M. D.; Pakstis, L.; Pochan, D. J.; Deming, T. J. *Nat. Mater.* **2004**, *3*, 244–248.
(30) Zhou, Y. F.; Yan, D. Y. *Angew. Chem., Int. Ed.* **2005**, *44*, 3223–3226.
(31) Wu, J.; Eisenberg, A. *J. Am. Chem. Soc.* **2006**, *128*, 2880–2884.
(32) Lomas, H.; Canton, I.; MacNeil, S.; Du, J. Z.; Armes, S. P.; Ryan, A. J.; Lewis, A. L.; Battaglia, G. *Adv. Mater.* **2007**, *19*, 4238–4243.
(33) Kishimura, A.; Koide, A.; Osada, K.; Yamasaki, Y.; Kataoka, K. *Angew. Chem., Int. Ed.* **2007**, *46*, 6085–6088.
(34) Shum, H. C.; Kim, J. W.; Weitz, D. A. *J. Am. Chem. Soc.* **2008**, *130*, 9543–9549.
(35) Yu, S. Y.; Azzam, T.; Rouiller, I.; Eisenberg, A. *J. Am. Chem. Soc.* **2009**, *131*, 10557–10566.

10.1021/ja1024063

of many technical challenges.[36−44] Lecommandoux et al. focused on embedding iron oxide nanoparticles (NPs) stabilized with a phosphoric diester type surfactant into the walls of vesicles formed by polybutadiene-*block*-poly-(glutamic acid) (PB-*b*-PGA) copolymers using a cosolvent self-assembly approach; they observed deformable vesicle-like membranes containing iron oxide NPs by transmission electron microscopy (TEM).[36,37] Armes et al. obtained gold-decorated vesicles formed by poly(ethylene oxide)-*block*-poly[2-(diethylamino)ethyl methacrylate-*stat*-3-(trimethoxysilyl) propyl methacrylate] [PEO-*b*-P(DEA-*stat*-TMSPMA)] copolymers using an in situ formation approach.[38,39] McCormick et al. obtained gold-decorated vesicles formed by poly[2-(dimethylamino) ethyl methacrylate-*block*-(*N*-isopropylacrylamide)] (PDMAEMA-*b*-PNIPAM) copolymers also using the in situ formation method.[40] Förster and co-workers focused on the incorporation of Fe_3O_4 NPs into the walls of vesicles formed by polyisoprene-*block*-poly(ethylene oxide) (PI-*b*-PEO) or poly(2-vinylpyridine)-*block*-poly(ethylene oxide) (P2VP-*b*-PEO) copolymers employing a film rehydration method; they obtained mostly multilamellar vesicles with Fe_3O_4 NPs as bridges between lamellae, and with occasional wall incorporation.[41] Binder and co-workers studied the embedding of gold or CdSe NPs into the walls of vesicles formed by polybutadiene-*block*-poly(ethylene oxide) (PB-*b*-PEO) copolymers also using the film rehydration method.[42,43] Maskos et al. investigated the encapsulation of CdSe/CdS/ZnS QDs into PB-*b*-PEO vesicle walls, again using the film rehydration method; they observed QDs inside the walls.[44] In many of these cases, the particles and the vesicle walls are of comparable size or, in some cases, comparable contrast. Therefore, it is frequently difficult from the EM micrographs to see the localization of the particles in any detail within the walls, i.e. to determine whether they are on or near the surface of the wall or how deeply below the surface they are located. In the case where the vesicle wall thickness is large enough relative to the particle size and the contrast is good, a more or less random distribution of the particles in the wall is observed.[39] The controlled localization of particles exclusively in the middle portion, i.e. central 10−20% of the vesicle wall, leaving the ca. 40−45% of the wall near both the internal and external interfaces free of particles, has not been achieved as yet.

It should be pointed out that a previous simulation[45] and subsequent experiments[46] on lamellar phases of diblock copolymers in bulk showed that the localization of polymer coated particles near the center of the polymer domain compatible with the particle surface coating is possible. It was suggested that localizing polymer coated particles near the center of the compatible polymer domain sacrifices th etranslational entropy of the particles but avoids an even larger chain stretching penalty incurred by distributing particles throughout the domain.[45,46]

Our group has explored the encapsulation of dendrimer molecules (G4-NH_2 PAMAM) into the walls of vesicles formed by polystyrene-*block*-poly(acrylic acid) (PS-*b*-PAA) copolymers, applying the cosolvent self-assembly method.[47,48] It was found that the dendrimer molecules combined with the PS-*b*-PAA copolymers in various proportions to form a range of aggregates, including hydrophobic "multiple dendrimer core micelles" with PS blocks on the outside, as well as hydrophilic "multiple dendrimer core inverse onion micelles" with hydrophilic PAA blocks as the outer corona covering an intermediate PS bridging layer; such structures were found to be embedded into the vesicle walls.[48]

Building on these results, we attempted to develop general methods of incorporating particles into the middle portion of vesicle walls. Our preliminary attempt involved electron dense NPs coated with a hydrophobic homopolymer, i.e. PS. The attempt was unsuccessful and led to precipitation or large compound micelle formation in contrast to the situation in bulk lamellar phases of block copolymers.[45,46] To force the NPs into the central portion of vesicle walls, in the next step, two types of electron dense NPs were prepared, both of which have a coating of diblock copolymers of the same or similar composition as the diblock used for the preparation of the vesicles. As Figure 1 shows, one type of NP consists of cross-linked Pb acrylate cores surrounded by PS_{155}-*b*-PEO_{45} coronas, i.e. PEO_{45}-*b*-PS_{155}-*b*-$P(APb)_{25}$ micelles, where $P(APb)_{25}$ denotes the cross-linked Pb acrylate in the micelle cores containing PAA chains of 25 units neutralized with Pb^{4+}; the other type of NP consists of gold nanoparticles (AuNPs) connected to a PS_{270}-*b*-PAA_{15} copolymer by a thioctate ester (TE) end group, i.e. TE-PS_{270}-*b*-PAA_{15} AuNPs. Since the protective polymers on the NPs were similar to those forming the vesicle walls, it appeared likely that the NPs should localize toward the center of the walls with the attached diblock copolymers partitioning to both interfaces. Both of these attempts were successful and, indeed, led to the localization of the NPs only in the central portion of vesicle walls. To the best of our knowledge, this represents the first case in which NPs, stabilized with block copolymers of the same type as those used to prepare the vesicles, were designed to be embedded into vesicle walls and were, indeed, localized in the central portion of the vesicle walls. The present paper reports the details of this study.

2. Experimental Section

The experimental details are given in the Supporting Information (pages S1−S8).

3. Results and Discussion

The characterization results of the synthesized polymers in this work are shown in the Supporting Information (pages S9−S14, Figures S1−S10).

3.1. Preparation and Characterizations of the Diblock Copolymer Coated NPs. The PEO_{45}-*b*-PS_{155}-*b*-$P(APb)_{25}$ micelles were prepared by cross-linking the PEO_{45}-*b*-PS_{155}-*b*-PAA_{25}

(36) Lecommandoux, S.; Sandre, O.; Chécot, F.; Rodriguez-Hernandez, J.; Perzynski, R. *Adv. Mater.* **2005**, *17*, 712–718.
(37) Lecommandoux, S.; Sandre, O.; Chécot, F.; Rodriguez-Hernandez, J.; Perzynski, R. *J. Magn. Magn. Mater.* **2006**, *300*, 71–74.
(38) Du, J. Z.; Armes, S. P. *J. Am. Chem. Soc.* **2005**, *127*, 12800–12801.
(39) Du, J. Z.; Tang, Y. Q.; Lewis, A. L.; Armes, S. P. *J. Am. Chem. Soc.* **2005**, *127*, 17982–17983.
(40) Li, Y. T.; Smith, A. E.; Lokitz, B. S.; McCormick, C. L. *Macromolecules* **2007**, *40*, 8524–8526.
(41) Krack, M.; Hohenberg, H.; Kornowski, A.; Lindner, P.; Weller, H.; Förster, S. *J. Am. Chem. Soc.* **2008**, *130*, 7315–7320.
(42) Binder, W. H.; Sachsenhofer, R.; Farnika, D.; Blaasb, D. *Phys. Chem. Chem. Phys.* **2007**, *9*, 6435–6441.
(43) Binder, W. H.; Sachsenhofer, R. *Macromol. Rapid Commun.* **2008**, *29*, 1097–1103.
(44) Mueller, W.; Koynov, K.; Fischer, K.; Hartmann, S.; Pierrat, S.; Basche, T.; Maskos, M. *Macromolecules* **2009**, *42*, 357–361.
(45) Thompson, R. B.; Ginzburg, V. V.; Matsen, M. W.; Balazs, A. C. *Science* **2001**, *292*, 2469–2472.
(46) Chiu, J. J.; Kim, B. J.; Kramer, E. J.; Pine, D. J. *J. Am. Chem. Soc.* **2005**, *127*, 5036–5037.
(47) Kroeger, A.; Li, X. F.; Eisenberg, A. *Langmuir* **2007**, *23*, 10732–10740.
(48) Li, X. F.; Kroeger, A.; Azzam, T.; Eisenberg, A. *Langmuir* **2008**, *24*, 2705–2711.

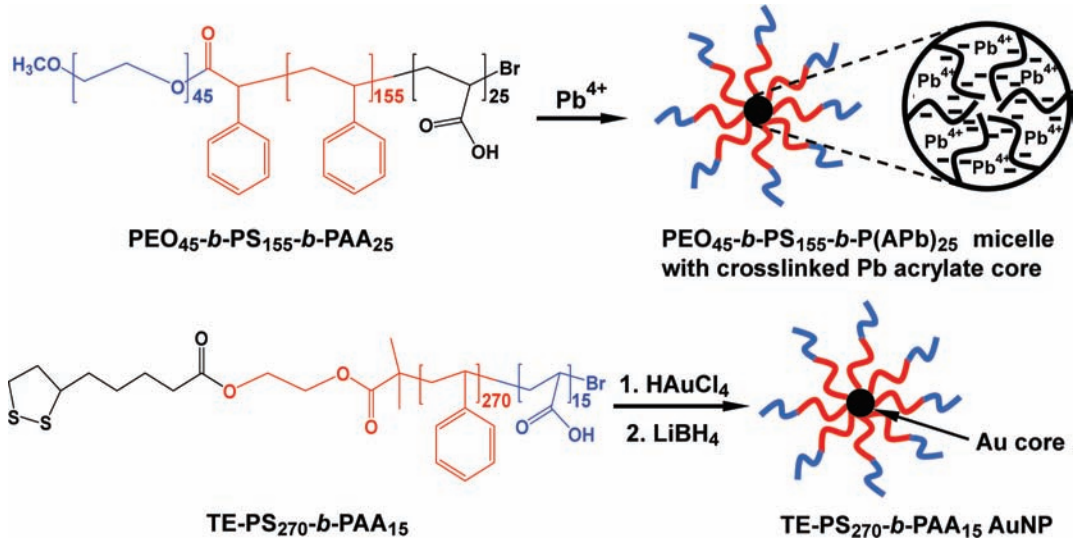

Figure 1. Schematic illustration of the preparation of the two types of diblock copolymer coated nanoparticles. In the structures of the nanoparticles, the red color indicates the hydrophobic PS blocks, and the blue color indicates the hydrophilic chains, i.e. the PEO or PAA blocks.

triblock copolymers with lead(IV) acetate, essentially following procedures given in the literature.[49,50] The cross-linking of PEO_{45}-*b*-PS_{155}-*b*-PAA_{25} molecules, as well as the removal of the unassociated PEO_{45}-*b*-PS_{155}-*b*-PAA_{25} copolymer, was confirmed using ^{1}H NMR spectra (Figure S11 in the Supporting Information), in which the proton peak, attributed to the carboxyl group, cannot be seen in the ^{1}H NMR spectrum of the PEO_{45}-*b*-PS_{155}-*b*-$P(APb)_{25}$ micelles, whereas it does appear in the spectrum of the PEO_{45}-*b*-PS_{155}-*b*-PAA_{25} copolymer. To determine the sizes of the cross-linked Pb acrylate cores and of the micelles, TEM and dynamic light scattering (DLS) studies were performed; the results are given in Figure S12 in the Supporting Information. The electron dense Pb acrylate cores have a high contrast for electrons and are clearly seen in the TEM photograph of the micelles. The average diameter of the cores obtained from the TEM images is 4.5 ± 1.1 nm. The DLS plot shows a single-peak distribution with an average hydrodynamic diameter (D_h) of 48 nm. This value is much larger than the 4.5 nm diameter of the cores because D_h, as measured by DLS in dioxane, includes the thickness of the PS-*b*-PEO corona surrounding the core. Each chain of this corona contains 200 repeat units or 445 backbone atoms, corresponding to an estimated unperturbed length of ca. 3 nm and a fully stretched length of ca. 56 nm. Subtracting the core diameter of 4.5 nm from the D_h value of 48 nm yields ca. 44 nm, corresponding to twice the corona dimension. The apparent size of the corona is, therefore, ca. 22 nm or somewhere between the unperturbed length and the fully stretched length of the corona chains. The value appears reasonable in view of the crowding near the micelle core. The NMR, TEM, and DLS results thus confirm the formation of the PEO_{45}-*b*-PS_{155}-*b*-$P(APb)_{25}$ micelles. The average aggregation number of the polymer chains in one micelle was estimated to be ca. 17 from the average core dimension; the calculation is given in section 2.5, pages S15−S16 in the Supporting Information.

The TE-PS_{270}-*b*-PAA_{15} AuNPs were prepared by reducing $HAuCl_4$ in a THF solution of TE-PS_{270}-*b*-PAA_{15} according to a method developed by Azzam et al.[51] The formation of TE-PS_{270}-*b*-PAA_{15} AuNPs was confirmed by TEM, UV−vis spectrometry, DLS, and thermogravimetric analysis (TGA) measurements. TEM results show that the AuNPs possess an average diameter of 4.0 ± 0.7 nm and a narrow size distribution (Figure S13a in the Supporting Information). The UV−vis spectrum exhibits an absorption peak of the AuNPs near $\lambda_{max} = 520$ nm (Figure S13b in the Supporting Information), which is a characteristic of small aggregation-free AuNPs.[51,52] It is well-known that the small aggregation-free AuNPs can be obtained preferentially when the AuNPs are protected by the attached organic chains after the reduction of $HAuCl_4$ in solution.[51,52] In the present case, the AuNPs are protected by the attached TE-PS_{270}-*b*-PAA_{15} copolymer chains. The DLS plot gives a single-peak distribution with an average D_h of 33 nm for the TE-PS_{270}-*b*-PAA_{15} AuNPs in dioxane (Figure S13c in the Supporting Information). As in the case of the PEO_{45}-*b*-PS_{155}-*b*-$P(APb)_{25}$ micelles, the D_h value is much larger than the 4 nm diameter of the Au cores obtained by TEM; the increase in size is due to the presence of the TE-PS_{270}-*b*-PAA_{15} copolymer chains on the surface of the AuNPs as the coronas, which are detected by DLS. Each chain of the TE-PS_{270}-*b*-PAA_{15} corona contains 285 repeat units, corresponding to an estimated unperturbed length of ca. 4 nm and a fully stretched length of ca. 71 nm. As before, subtracting the core diameter of 4 nm from the D_h value of 33 nm yields 29 nm, corresponding to twice the corona dimension. Thus, the apparent size of the corona is ca. 15 nm, which is between the unperturbed length and the fully stretched length of the corona chains. TGA shows that the content of the gold in the TE-PS_{270}-*b*-PAA_{15} AuNPs is ca. 13 wt %, while the other ca. 87 wt % is from the TE-PS_{270}-*b*-PAA_{15} copolymer (Figure S13d in the Supporting Information). According to TEM and TGA results, the average number of TE-PS_{270}-*b*-PAA_{15} copolymer chains associated with one AuNP is estimated to be ca. 90; the calculation is shown in section 2.6, page S17 in the Supporting Information.

(49) Moffitt, M.; McMahon, L.; Pesse1, V.; Eisenberg, A. *Chem. Mater.* **1995**, *7*, 1185–1192.
(50) Duxin, N.; Liu, F.; Vali, H.; Eisenberg, A. *J. Am. Chem. Soc.* **2005**, *127*, 10063–10069.
(51) Azzam, T.; Eisenberg, A. *Langmuir* **2007**, *23*, 2126–2132.
(52) Corbierre, M. K.; Cameron, N. S.; Sutton, M.; Mochrie, S. G. J.; Lurio, L. B.; Rühm, A.; Lennox, R. B. *J. Am. Chem. Soc.* **2001**, *123*, 10411–10412.

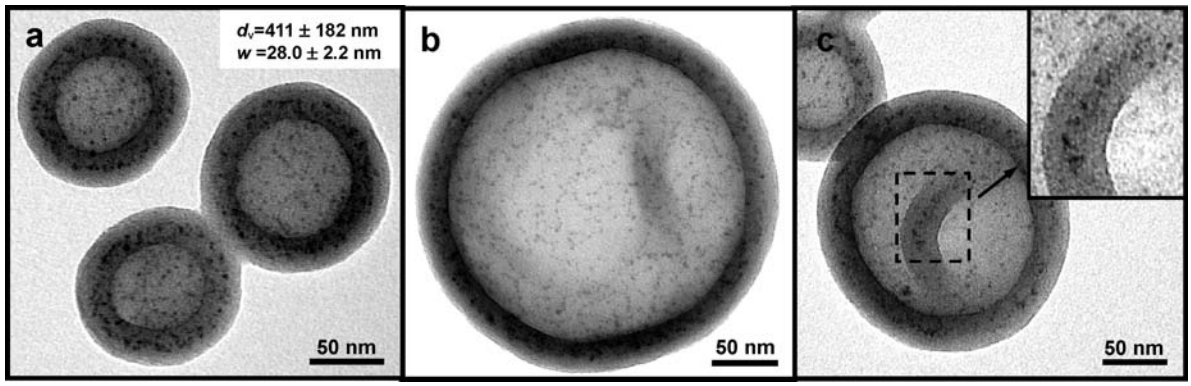

Figure 2. TEM micrographs of the vesicles with the incorporated nanoparticles prepared from the combined solution of the PS_{235}-*b*-PEO_{45} copolymer (0.5 wt %) and the PEO_{45}-*b*-PS_{155}-*b*-$P(APb)_{25}$ micelles (0.5 wt %). (a) Small vesicles; (b) a large vesicle; (c) an indented vesicle; the magnified indentation of the vesicle is shown in the inset.

3.2. Controlled Incorporation of the NPs into Vesicle Walls. Before attempting the incorporation of the NPs, vesicles were prepared from the vesicle former alone, i.e. the PS_{235}-*b*-PEO_{45} copolymer or the PS_{310}-*b*-PAA_{47} copolymer, respectively. The average diameter (d_v) and wall thickness (w) of the PS_{235}-*b*-PEO_{45} vesicles, obtained by measuring 100−200 vesicles in TEM photographs, are 400 ± 130 nm and 28.8 ± 2.5 nm, respectively. The d_v and w of the PS_{310}-*b*-PAA_{47} vesicles are 131 ± 36 nm and 28.7 ± 1.9 nm, respectively. Typical TEM photographs of these vesicles are shown in Figure S14 in the Supporting Information. Some large vesicles show indentations, which are possibly induced by an osmotic effect during the water addition to the dioxane solution of the copolymers.

The incorporation of the PEO_{45}-*b*-PS_{155}-*b*-$P(APb)_{25}$ micelles into the walls of both PS_{235}-*b*-PEO_{45} and PS_{310}-*b*-PAA_{47} vesicles was carried out by the dropwise addition of water into the combined dioxane solutions of the PS_{235}-*b*-PEO_{45} or PS_{310}-*b*-PAA_{47} copolymers and the preformed electron dense micelles. In the combined solutions, the initial concentrations of the vesicle formers were 0.5 wt %; the initial concentrations of the micelles, based on rough estimates, were 0.13, 0.25, and 0.5 wt %, respectively. Other concentrations were not explored. All references to loading levels in the text refer to weight percentages in the mixed solutions prior to the formation of the vesicles. It should also be stressed here that the incorporation of the NPs occurred during the formation of the vesicles, not by penetration of the NPs into the formed vesicle walls, a process which would be highly unlikely. Figure 2 shows the TEM photographs of the vesicles prepared from the 0.5 wt %/0.5 wt % combined solution of the PS_{235}-*b*-PEO_{45} copolymer and the micelles. The average diameter and wall thickness of the vesicles are given in the upper right corner of Figure 2a. The TEM image of the vesicles prepared from the 0.5 wt %/0.5 wt % combined solution of the PS_{310}-*b*-PAA_{47} copolymer and the micelles is shown in Figure S15 in the Supporting Information. In the TEM images, such as those in Figure 2, a large number of black Pb acrylate cores can be seen as black dots in the vesicles. As can be expected, the number density of the Pb cores in the vesicles decreases with decreasing initial concentration of the micelles in solution. When the concentration of the micelles in solution is reduced to ca. 0.13 wt %, only a few black dots can be seen in the vesicles (micrographs not shown). Most importantly, for all reasonable concentration ratios, no black dots can be seen in the outer ca. half section of the vesicle walls, as is clearly shown in Figure 2, which gives typical examples of small, large, and indented vesicles. We refer to the thickness of the empty section as the "empty distance". By contrast, it is known that if the NPs are randomly distributed in the vesicle wall[39] or on the surface of the vesicle wall,[53] no such empty distance is seen; i.e. the NPs can be seen everywhere in the vesicle in the TEM image, including the outer half section of the wall.[39,53] In this work, the empty distances, which are close to half the thicknesses of the vesicle walls, are seen in all of the vesicles containing the NPs (both the Pb acrylate cores and the AuNPs to be discussed later) in the TEM images. Obviously, this is not accidental. Besides, it is well-known that, in TEM studies, the placement of the vesicles on TEM grids cannot be controlled, so that the vesicles are oriented randomly on TEM grids. Therefore, the empty distance should be independent of the orientation of the vesicles. This was also confirmed by tilting studies in TEM (Figure S16 in the Supporting Information).

While TEM images provide direct evidence of an empty distance on the outside of the vesicle walls, two lines of evidence can be cited to suggest that a similar empty distance also exists on the inside of the walls; i.e. the NPs are localized only in the central portion of the walls. One line of evidence comes from TEM images of indented vesicles, such as that shown in Figure 2c. It should be remembered that, for topological reasons, the outer portion of the convex side of an indentation originates from what was the concave side prior to indentation, i.e. the interior of the vesicle wall (Figure S17 in the Supporting Information). Clearly, the convex side of the indentation also shows the presence of an empty distance, which proves that the empty distance is present on both internal and external interfaces of the vesicle wall. Another argument in favor of the existence of the empty distance on both interfaces of the vesicle walls is based on consideration of symmetry, as shown in Figure 3, which schematically illustrates two possible types of wall incorporation. The upper half on the right of Figure 3 shows the situation of each NP located in the central portion of the wall, with the corona chains extended more or less equally toward each interface. The aggregates in the wall are drawn with the hydrophilic segments of the protective diblocks in the water phase, along with the hydrophilic segments of the vesicle forming diblocks. The lower half on the right of Figure 3 illustrates the situation for the asymmetric placement of the NPs, i.e. a structure in which all of the corona chains are pointing only to one side of the NP and, for any one NP, are extended to either the inside or outside interface, but not to both. Such a

(53) Wang, M. F.; Zhang, M.; Siegers, C.; Scholes, G. D.; Winnik, M. A. *Langmuir* **2009**, *25*, 13703–13711.

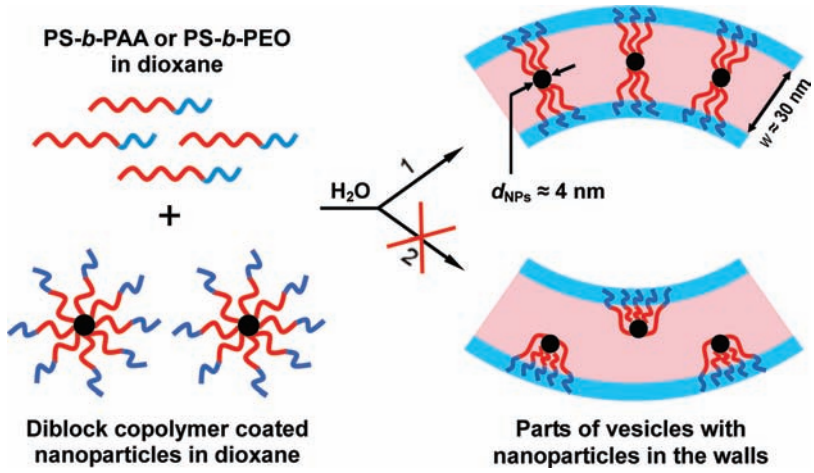

Figure 3. Schematic illustration of two possible types of incorporation of the diblock copolymer coated nanoparticles into vesicle walls. The red color represents the hydrophobic composition, and the blue color represents the hydrophilic composition. Possibility 2 is believed to be highly unlikely.

unilateral segregation is highly unlikely, for both entropic and steric reasons, so that the placement of the NPs in the central portion of the wall appears most reasonable. In addition, it can be calculated that the unperturbed length of the PS blocks in the PEO_{45}-*b*-PS_{155}-*b*-$P(APb)_{25}$ micelles is ca. 2 nm, while the fully stretched length of the PS blocks is ca. 39 nm. As given on the right section of Figure 3, the average wall thickness of the vesicles is ca. 30 nm, while the average size of the NPs is ca. 4 nm. Thus, if the NPs are located in the middle of the vesicle walls, the distance that the PS blocks on the NPs in the walls have to span is ca. $(30 - 4)/2 = 13$ nm, which is between the unperturbed length and the fully stretched length of the PS blocks on the NPs; this distance appears reasonable in view of the crowding of the PS blocks within the vesicle walls. Finally, with a vesicle radius of ca. 50−300 nm, the effect of wall curvature on the placement of a ca. 4 nm sphere is probably negligible. Therefore, it is reasonable to expect that the NPs should be located in the central portion of the vesicle walls, leading to the presence of the empty distance on both sides of the walls.

As with the Pb containing micelles, the incorporation of the AuNPs into the walls of the PS_{310}-*b*-PAA_{47} vesicles was carried out by the dropwise addition of water into the combined dioxane solutions of the PS_{310}-*b*-PAA_{47} copolymer and the TE-PS_{270}-*b*-PAA_{15} AuNPs. In the combined solutions, the initial concentrations of the vesicle former were also 0.5 wt %; the initial concentrations of the TE-PS_{270}-*b*-PAA_{15} AuNPs, based on rough estimates, were 1.2, 2.5, and 5 wt %, respectively. Other concentrations were not explored. In this case, when the concentration of the TE-PS_{270}-*b*-PAA_{15} AuNPs was 2.5 or 5 wt %, precipitation occurred after the addition of water, along with the formation of some other aggregates; vesicles were not observed. This was not further investigated in this work. When the concentration of the TE-PS_{270}-*b*-PAA_{15} AuNPs was 1.2 wt % in the original mixed solution, vesicles with the internalized AuNPs were obtained. A typical TEM image of the vesicles with the internalized AuNPs is shown in Figure S18 in the Supporting Information; more TEM images, along with the theoretical and fitted curves to be discussed later, are shown in Figure S22 in the Supporting Information. As in the vesicles containing Pb acrylate cores, the AuNPs are also absent from the outer ca. half portion of the vesicle walls in the TEM images. For the same reasons discussed in the previous two paragraphs, the AuNPs are also considered to be localized in the central portion of the vesicle walls.

The NPs (Pb or Au) are expected to be randomly distributed in a thin spherical layer or shell going through the middle of the vesicle wall. Theoretically, by considering the projection of the spherical vesicle containing the NPs onto a plane, one can calculate the radial distribution of the NPs in a vesicle in the TEM micrograph, which represents a two-dimensional projection. A theoretical equation of the radial distribution of the NPs was derived as part of this work (section 2.8.1, pages S20−S22 in the Supporting Information), as shown in eq 1, which gives the cumulative percentage of the NPs as a function of the increasing radial distance from the outer edge toward the center of the vesicle; the equation is

$$p = \frac{\sqrt{(R_v - a)^2 - (R_v - d)^2}}{(R_v - a)} \times 100 \qquad (1)$$

where p is the cumulative percentage, R_v is the radius of the vesicle, a is the empty distance, and d is the increasing radial distance from the outer edge toward the center of the vesicle (d is variable and $a \le d \le R_v$). The derivation of the equation is based on an idea that the particles are randomly located in a thin spherical layer, which goes through the middle of the vesicle wall (Figure S19 in the Supporting Information); the number of the particles projected within an annulus onto the equatorial plane (or onto the micrograph) is equal to the number of the particles in the spherical layer in the middle of the vesicle wall located directly above and below the annulus, i.e. a "belt" on both sides of the "equator" around the spherical layer containing the particles, the projection of which onto the equatorial plane is the annulus. Since the particles are randomly distributed in the spherical layer, the percentage of the particles projected within the annulus is simply related to the percentage of the surface area of the belt relative to that of the spherical layer containing the particles. To obtain the percentage, one needs to integrate over the surface area of the belt. According to eq 1, the theoretical curve can be drawn once the empty distance (a) is known from the experimental data, as discussed below.

Experimentally, to determine the radial distribution of the NPs in a vesicle in the micrograph, we measured the radial distances from each AuNP in a vesicle to the nearest point on

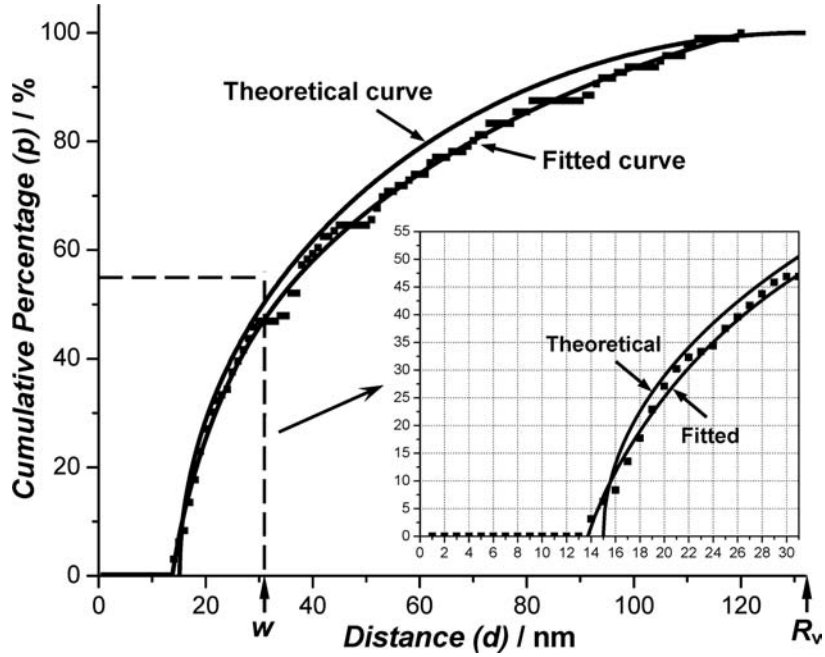

Figure 4. Plot of the cumulative percentage of the AuNPs in a vesicle as a function of the increasing radial distance from the outer edge toward the center of the vesicle. The radius (R_v) of the vesicle is 132 nm, and the wall thickness (w) is 31 nm.

the outer edge of the vesicle in the TEM image (Figure S20 in the Supporting Information). From the data, the experimental plot of the cumulative percentage of the AuNPs as a function of the increasing radial distance from the outer edge toward the center of the vesicle was obtained, as shown in Figure 4. The detailed procedure to obtain the plot is described in section 2.8.1, pages S22−S24 in the Supporting Information. As can be seen in Figure 4, the cumulative percentage is zero in the first ca. 14 nm of the plot, which indicates that the corresponding section of the vesicle is devoid of AuNPs; i.e. the empty distance is ca. 14 nm.

At this point, it should be emphasized that the empty distance cannot be the thickness of the hydrophilic (PAA or PEO) shell around the vesicle wall. First of all, it is known that the electron contrast of PAA or PEO is much lower than that of PS, so that the PAA or PEO shell is not visible in TEM micrographs. Second, in this case, given that the PS_{310}-b-PAA_{47} copolymer is the vesicle former, the thickness of the PAA shell can be only ca. 1.5 nm (half of the wall thickness of ca. 30 nm times the volume fraction (ca. 0.1) of the PAA block in the diblock), while the empty distance is ca. 14 nm. Thus, the empty section of the vesicle wall is 10 times larger and therefore cannot be identified with the PAA shell, even if the latter were visible in TEM micrographs. Since the empty distance cannot be the thickness of the hydrophilic shell, the TEM image and the plot in Figure 4 indicate that the outer ca. 14 nm thick portion of the vesicle wall on the TEM image is devoid of AuNPs.

Once the empty distance, i.e. the parameter a in eq 1, is known to be ca. 14 nm from the experimental plot, the theoretical curve can be drawn. In calculating the curve, a is allowed to vary by ±1 nm to optimize the fit over the entire experimental plot; the best result is obtained with $a = 15$. The result, i.e. the theoretical curve, is shown in Figure 4, where one can compare the experimental result with the theory. For improved precision in determining the empty distance, the experimental points were fitted empirically using Origin software. The fitted curve is also shown in Figure 4. Equation 2 is the result of the fit.

$$p = 117.6 - 105.3 \times \exp(-d/67.9) - 157.2 \times \exp(-d/8.3) \quad (2)$$

It should be mentioned that this equation is only valid for the vesicle used for Figure 4, i.e. the same vesicle as shown in Figure S20 in the Supporting Information; for other vesicles in the micrographs, the fitted equations are similar, differing only in the numerical values of the constants. The empty distance thus obtained from an extrapolation of the fitted curve for this vesicle is ca. 14 nm. Since the vesicle wall is 31 nm thick and the empty distance exists on both internal and external interfaces of the wall, it appears that the AuNPs are, within the level of approximation, located within a spherical layer of ca. 3 nm (31 − 2 × 14), i.e. central ca. 10% of the wall. It should be recalled that the average size of the NPs is ca. 4 nm. Therefore, the 3 nm thickness should be taken only as an approximation to the central localization of the AuNPs. The curves and results for three additional vesicles are given in Figure S22 in the Supporting Information.

Another qualitative model of the relative radial darkness of various regions in a vesicle with internal NPs on the micrograph is based on the idea that the particles can be represented as a continuous gray thin spherical layer going through the middle of the vesicle wall (Figure S23 in the Supporting Information). The electron absorbing power of the particle layer is assumed to be uniform and greater than that of the PS, but not infinite. The overall electron absorption of such a structure is equivalent to that of two concentric vesicles. The profile contributed by the vesicle itself is shown by the green curve, that of the concentric particle layer by the red curve, and the sum by the blue curve. While the electron micrograph does not have enough resolution to allow for a quantitative fit, it is clear that the inner edge of the vesicle wall is the darkest, as can be observed in many micrographs. Other regions of interest are indicated by arrows both on the model and on the micrograph of the vesicle.

This work provides a general method for the incorporation of particles into the central portion of vesicle walls. Such incorporation is expected to be useful, if the particles need to be protected on all sides by the hydrophobic wall-forming material, e.g. in labeling or catalytic applications. For example, a ca. 10 nm organic (e.g., PS) layer, which is easily and rapidly penetrated by small organic molecules, but with much more difficulty by inorganic ions, would provide some barrier to inorganic ions, which might poison the catalyst, at only a slight cost in overall speed of reaction. In addition, the central localization would provide equal protection for all the particles, rather than having some more exposed to the potentially toxic environment than others if the particles were randomly located within the wall. Finally, the central localization would prevent detachment of the particles from the vesicle surface under rough handling, if the particles were located on or near the surface.

4. Conclusions

This paper describes the controlled incorporation into only the central portion of the vesicle walls of two types of electron dense NPs, which have a coating of diblock copolymers of the same or similar composition as that of the diblock used for the preparation of the vesicles; one type of NP consists of cross-linked Pb acrylate cores surrounded by the PS_{155}-*b*-PEO_{45} coronae, while the other consists of AuNPs stabilized with the PS_{270}-*b*-PAA_{15} copolymer (Figure 1). TEM micrographs show that the empty distances, which are close to half the thicknesses of the vesicle walls, are present in all of the vesicles with the internalized NPs. TEM micrographs of indented vesicles (Figure 2c) supported by the argument on the symmetrical placement of the NPs in the vesicle walls (Figure 3) demonstrate the existence of the empty distance on both interior and exterior interfaces of the walls, i.e. the central localization of the NPs in the walls. The radial distribution of the NPs in the vesicles in the TEM images is also studied. The theoretical and experimental curves of the radial distribution are obtained (Figure 4). From the curves, it is calculated that the NPs are localized in the central 10−20% of the vesicle walls.

Acknowledgment. The authors would like to thank Tony Azzam, Shaoyong Yu, and Qinghua Wu for useful suggestions and help in this work. The authors would also like to acknowledge financial support from the Natural Science and Engineering Research Council of Canada (NSERC).

Supporting Information Available: The contents of the Supporting Information include the experimental section, characterizations of the prepared polymers and NPs, all of the calculations and models mentioned in this paper, and more TEM micrographs, among others. This material is available free of charge via the Internet at http://pubs.acs.org.

JA1024063